Protein–Protein Interactions

International Edition: DOI: 10.1002/anie.201601299
German Edition: DOI: 10.1002/ange.201601299

One-Pot N2C/C2C/N2N Ligation To Trap Weak Protein–Protein Interactions

*Lei Zhao, Christiane Ehrt, Oliver Koch, and Yao-Wen Wu**

Abstract: *Weak transient protein–protein interactions (PPIs) play an essential role in cellular dynamics. However, it is challenging to obtain weak protein complexes owing to their short lifetime. Herein we present a general and facile method for trapping weak PPIs in an unbiased manner using proximity-induced ligations. To expand the chemical ligation spectrum, we developed novel N2N (N-terminus to N-terminus) and C2C (C-terminus to C-terminus) ligation approaches. By using N2C (N-terminus to C-terminus), N2N, and C2C ligations in one pot, the interacting proteins were linked. The weak Ypt1:GDI interaction drove C2C ligation with $t_{1/2}$ of 4.8 min and near quantitative conversion. The Ypt1-GDI conjugate revealed that binding of Ypt1 G-domain causes opening of the lipid-binding site of GDI, which can accommodate one prenyl group, giving insights into Rab membrane recycling. Moreover, we used this strategy to trap the KRas homodimer, which plays an important role in Ras signaling.*

Protein–protein interactions (PPIs) are fundamental for most cellular processes.[1] protein–protein interactions form dynamic interaction networks that connect different cellular processes.[2] Depending on the half-life of protein complexes, protein–protein interactions can be categorized into permanent and transient forms.[3] More frequently, transient protein–protein interactions play essential roles in regulating intracellular dynamic processes, such as signal transduction and cell cycle transition. In most cases, transient protein–protein interactions are weak interactions with $K_d > \mu M$ and short half-life in a range of minutes or seconds.[4] Elucidation of these interactions is crucial for unraveling signaling networks and the development of therapeutic protein–protein-interaction inhibitors.[5] Owing to their short lifetime, the detection of and access to weak transient protein complexes remain challenges.[6]

Two major classical strategies to obtain weak protein complexes include chemical cross-linking and fusion proteins.[7] Chemical cross-linking involves the covalent connecting of interacting proteins using bifunctional reagents or disulfide bond.[8] This technique requires knowledge of the key amino acid residues involved in binding. Mutagenesis studies are therefore required. Moreover, because cross-linking reagents react with amine and sulfhydryl moieties, which are abundant in proteins, non-specific reactions leading to oligomerization are often observed.[9] The fusion protein strategy using Gly-rich linkers is rather straightforward. However, the orientation of a protein in the complex is unknown. Optimization of linker lengths for each condition is necessary, so that the linker does not interfere with the interactions of the binding partners.[10] Design of such linkers usually requires structural knowledge of at least one of the interaction partners and binding information to obtain a preliminary model of the complex. Unbiased and facile methods for trapping weak protein–protein interactions remain forthcoming.

Native chemical ligation (NCL) and expressed protein ligation (EPL) are powerful techniques for chemical synthesis of proteins.[11] We reasoned that a weak protein interaction could increase the interaction probability of the termini from both proteins, thereby facilitating chemical protein ligation and trapping the transient protein complexes in an unbiased manner. Statistically, there will be four possibilities to link two proteins at termini. The conventional N-terminal to-C-terminal (N2C) ligation only covers half of them (Scheme 1 A). To expand the ligation methods, we establish novel strategies, named protein N-terminal to N-terminal (N2N) ligation and protein C-terminal to C-terminal (C2C) ligation (Scheme 1 B).

Rab GTPases play an important role in regulating the vesicular trafficking of intracellular membranes.[12] Ypt (Yeast

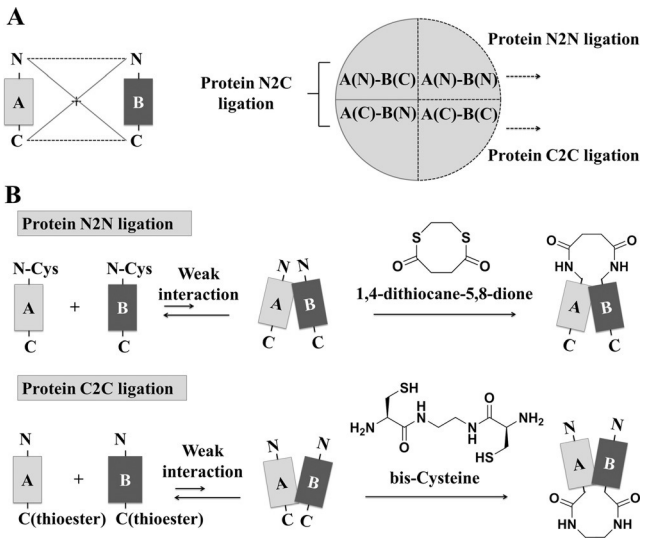

Scheme 1. A) The pattern of terminal protein ligations. B) Strategies for generating protein complexes by N2N and C2C ligation.

[*] Dr. L. Zhao, Dr. Y.-W. Wu
Chemical Genomics Center of the Max Planck Society
Otto-Hahn-Strasse 15, 44227 Dortmund (Germany)
E-mail: yaowen.wu@mpi-dortmund.mpg.de
C. Ehrt, Dr. O. Koch
TU Dortmund University, Faculty of Chemistry and Chemical Biology
Otto-Hahn-Strasse 6, 44227 Dortmund (Germany)

Supporting information for this article can be found under: http://dx.doi.org/10.1002/anie.201601299.

protein transport) is a Rab homologue in yeast. Rab proteins require prenylation to associate with membranes. In the Rab cycle, GDP dissociation inhibitor (GDI), extracts the prenylated GDP-bound Rab from the membrane. GDI binds to unprenylated Rab in low affinity (K_d of μM), while it binds to prenylated Rab in much higher affinity (K_d of nM). The difference in binding energy is the thermodynamic driving force of the GDI-mediated extraction of Rab from membranes.[13] However, the molecular mechanism of Rab membrane recycling remains elusive. This study was impeded largely due to the difficulty of obtaining unprenylated Rab:GDI binding intermediates because of the low affinity. Herein, we present a general strategy to trap weak protein–protein interactions using N2C, N2N and C2C chemical protein ligation approaches.

To achieve N2N and C2C ligations, a thioester moiety and 1,2-aminothiol need to be incorporated at the N- and C-terminus of the protein, respectively. To this end, we designed and prepared bifunctional molecules, that is, 1,4-dithiocane-5,8-dione (DT) and bis-cysteine (bis-Cys; Scheme 1B, Supporting Information). Ypt1-thioester, GDI-thioester, N-Cys-Ypt1 and N-Cys-GDI were prepared through intein-chemistry and Tobacco Etch Virus (TEV) protease-mediated cleavage, respectively (Figure S1,S2 in the Supporting Information).[14] 1–3 mM DT was incubated with 100–300 μM N-Cys-GDI to install the thioester moiety at the protein N-terminus (N-thioester-GDI) with a conversion rate of approximately 99% (Figure S3,S4). 1–3 mM bis-Cys (BC) was ligated with 100–300 μM Ypt1-thioester or GDI-thioester to introduce the 1,2-aminothiol moiety at the protein C-terminus (Ypt1-BC or GDI-BC) with nearly quantitative conversion (Figure S3,S4). To quickly determine whether the ligation strategies could efficiently trap the weak protein–protein interaction and facilely identify the most favorable one (Table 1), we carried out all reactions in one pot. Two Ypt1 derivatives (Ypt1-thioester, N-Cys-Ypt1) and four GDI derivatives (GDI-thioester, GDI-BC, N-Cys-GDI, N-thioester-GDI) were mixed in the same molar ratio. The trapped covalent protein complex was clearly identified by MALDI-TOF and denaturing SDS-PAGE (Figure S5,S6).

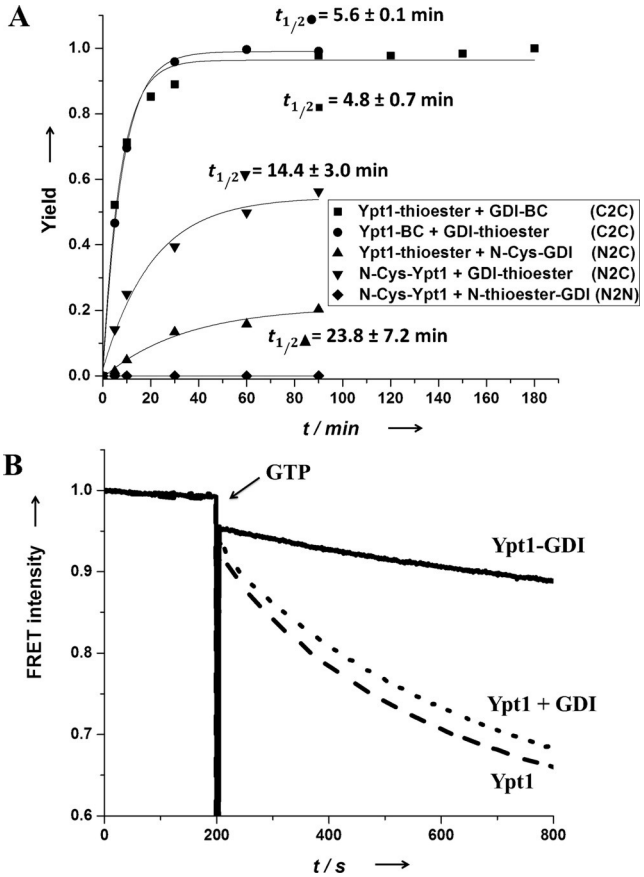

Figure 1. A) Time-course of N2C, N2N, and C2C ligations. The progression curves were fitted according to single-exponential function to calculate the reaction half-life ($t_{1/2}$). BC = bis-Cys. B) Measurement of nucleotide exchange by FRET. Excitation: 298 nm, Emission: 440 nm. 1 μM Mant-GDP-bound Ypt1-GDI conjugate or 1 μM Mant-GDP-bound Ypt1 in the absence and the presence of 1.2 μM GDI was used.

Table 1: Different ligation strategies to prepare Ypt1-GDI conjugates.[a]

	Ypt1-thioester	Ypt1-BC	N-Cys-Ypt1
GDI-thioester	–	n-Ypt1-GDI-n (C2C) yield 94% $t_{1/2}$ = 5.6 min	n-GDI-n-Ypt1 (N2C) yield 54% $t_{1/2}$ = 14.4 min
GDI-BC	n-Ypt1-GDI-n (C2C) yield 98% $t_{1/2}$ = 4.8 min	–	–
N-Cys-GDI	n-Ypt1-n-GDI (N2C) yield 21% $t_{1/2}$ = 23.8 min	–	–
N-thioester-GDI	–	n.d.	Ypt1-n-n-GDI (N2N) n.r.

[a] The methods are marked in brackets. "n" refers to the N-terminus of the protein. n.d.: not determined. n.r.: no observed reaction.

Encouraged by the result of the one-pot reaction, the four ligation modes were carried out individually. To take advantage of the weak protein–protein interaction as a template for the ligation, we used high concentrations of both proteins (100–300 μM) above K_d value (37.3 μM, Figure S7). Only C2C ligation led to high yields and remarkable high reaction rates with $t_{1/2}$ of approximately 5 min and nearly quantitative conversion (Figure 1A, Figure S8). In contrast, N2C ligations proceeded much slower with lower yield (< 50%) (Figure 1A, Figure S9). The N2N ligation did not yield the product, whereas the N-thioester-GDI readily ligated with cysteine (Figure S4C,S9). Therefore, the weak binding of Ypt1:GDI determines the orientation of both termini, resulting in varied yields and reaction rates of different ligations (Table 1). In this case, Ypt1:GDI binding brings both C-termini in proximity to facilitate efficient C2C ligation, which quantitatively trapped the Ypt1-GDI complex (Scheme S1, Figure S10). If none of the termini are close enough to confer efficient ligation, an appropriate linker (e.g. GGS repeat) could then be genetically introduced to the terminus of one of the

binding partners. One-pot ligation strategy can be used to evaluate the linker.

These observations on the reaction efficiencies of different ligation modes are consistent with the crystal structure of prenylated Ypt1:GDI complex.[15] The N-terminus of GDI is located at the opposite side of both termini of Ypt1 (Figure S11). Consequently, N2N (Ypt1-n-n-GDI) and N2C (n-Ypt1-n-GDI) ligations essentially do not work. However, the C-terminus of GDI is located close to the Ypt1 termini (Figure S11). The last visible residue GDI^{Q446} at the C-terminus is approximately 22 Å and approximately 17 Å away from the first visible N-terminal residue $Ypt1^{S3}$ and the last C-terminal residue $Ypt1^{L193}$ involved in GDI binding, respectively. The C-terminal residues downstream of the C-terminal interaction motif (CIM) consisting of V^{191} and L^{193} residues that form hydrophobic interactions with GDI, are largely flexible.[16] Based on this knowledge, we simulated the flexible conjugated peptide fragments linking GDI C-terminus with Ypt1 *N*- and C-termini based on the prenylated Ypt1:GDI complex structure (PDB: 2BCG) using a molecular dynamics (MD) simulation approach. Modelling of n-GDI-n-Ypt1 and n-Ypt1-GDI-n conjugates suggested that the conformation of the linker peptide of the C2C-ligated product is relatively flexible, while the linker of the N2C-ligated product is rather rigid (Figure 2). This scenario results from the sufficiently long linker in the C2C-ligated product and the short linker in the N2C-ligated product, which is not long enough to span the native distance between the Ypt1 N-terminus and the GDI C-terminus. This is in keeping with the ligation efficacies for both ligation reactions (Figure 1 A). Previous research also

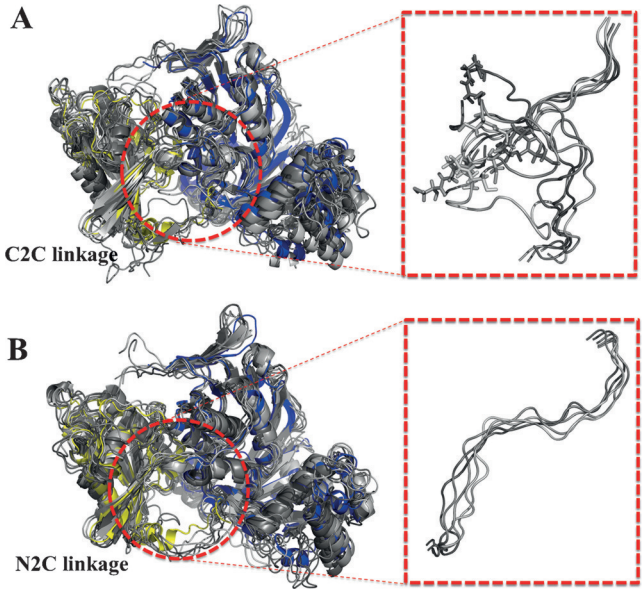

Figure 2. Molecular dynamics simulation snapshots of A) C2C and B) N2C ligated Ypt1-GDI complexes aligned to the crystal structure of doubly prenylated Ypt1:GDI complex (PDB code: 2BCG). MD simulation frames were clustered and five resulting representative structures are shown in gray. The representative of the conformational cluster with the highest number of frames is shown in dark gray (Table S1). The crystal structures of Ypt1 and GDI are colored in yellow and blue, respectively. The linkers of Ypt1 and GDI are highlighted in red boxes. Bis-Cys is shown in stick mode.

suggested that a flexible linker is required to observe the weak interaction between Tudor domain and methylated arginine.[17] Consequently, the N2C ligation constrains the protein complex, which is translated into disruption of the binding between the conserved G4 motif (NKxD) and GDP in Ypt1 (Figure S12). To observe conformational changes on GDI after C2C ligation, the unligated Ypt1:GDI, apo-GDI and C2C-ligated Ypt1:GDI were subjected to MD simulation. Interestingly, α-helix D (residues 129–137) that constitutes the prenyl-binding site of GDI undergoes significant conformational change after C2C ligation (Figure S13). Dictionary of Secondary Structure of Proteins (DSSP) analysis showed that this region adopts largely α-helical configuration in the unligated Ypt1:GDI and in apo-GDI, while it is disordered in the C2C-ligated conjugate (Figure S13 C), indicating that the lipid-binding site of GDI is regulated by the Ypt1 interaction.

We further demonstrated the specificity of the reaction. Rab1, the mammalian homologue of Ypt1, which does not bind to yeast GDI, did not show significant C2C ligation with GDI (Figure S14). Furthermore, because GDI only binds to GDP-bound Rab but not GTP-bound Rab,[18] we examined the nucleotide dependency of the reaction. In contrast to GDP-bound Ypt1, the GppNHp (non-hydrolyzable GTP analogue)- or GMP-bound Ypt1 showed significantly lower reaction rates and poor yields (Figure S15). These results suggest that the efficient ligation is driven by the Ypt1:GDI interaction.

Next, we characterized the C2C-ligated Ypt1-GDI conjugate. GDI inhibits the release of bound nucleotide when binds to prenylated Rab.[19] We carried out fluorescence resonance energy transfer (FRET)-based nucleotide-exchange assays using Mant-GDP (Figure S16). Mant-GDP:Ypt1 readily underwent nucleotide exchange upon addition of excess GTP in the absence or the presence of GDI, whereas nucleotide exchange was retarded in the Ypt1-GDI conjugate (Figure 1 B, Figure S17). These results suggest that C2C ligation trapped the native Ypt1:GDI interaction. Therefore, GDI can exert its inhibitory function on GDP dissociation as it does on prenylated Ypt1.[20]

With the establishment of a covalent Ypt1-GDI complex, we are able to further understand the function of GDI in Rab membrane recycling. One of the intriguing questions is how GDI extracts prenylated Rab from the membrane. Structures of prenylated Ypt1:GDI complexes show that α-helix D of GDI moves outwards to form the lipid-binding groove that is not observed in apo-GDI.[13a,15] The formation of lipid-binding site is induced either by interaction with the GTPase domain or by the docking of the C-terminal prenyl moiety of Ypt1.[13a] To distinguish these two scenarios, the intermediate unprenylated Ypt:GDI complex is required, which can be ideally emulated by the Ypt1-GDI conjugate. The MD simulation suggested that α-helix D of GDI could undergo conformational change upon Ypt1 binding. We used isothermal titration calorimetry (ITC) to measure the interaction of the prenyl group, geranylgeranylated cysteine (CysGG), with proteins (Figure 3). The results showed that CysGG only interacts with Ypt1-GDI ($K_d = 14.6$ μM) but not with Ypt1 or GDI alone. CysGG was also titrated to a mixture of 50 μM

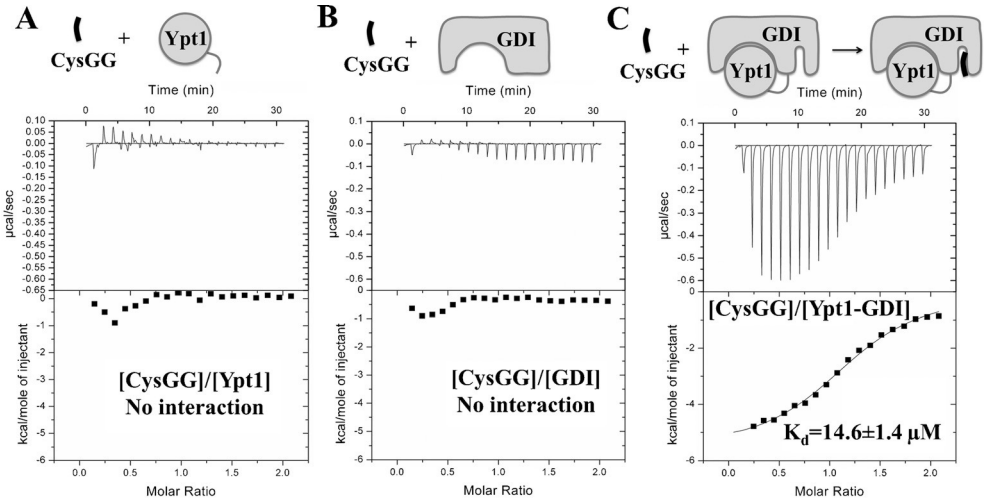

Figure 3. ITC measurements of the titration of CysGG to the Ypt1-GDI conjugate, Ypt1, or GDI.

Ypt1 and GDI. The interaction was much weaker than the covalent Ypt1-GDI complex ($K_d = 61$ µM; Figure S18), suggesting the formation of the lipid-binding site to a lesser extent, in line with the transient nature of the Ypt1:GDI interaction.[21] These results demonstrated that binding of the Ypt1 G-domain to GDI is sufficient to induce conformational changes on GDI leading to opening of the lipid-binding site. Moreover, the ITC measurements showed that the stoichiometry of the interaction between CysGG and Ypt1-GDI is 1:1, suggesting that the opened groove can only stably accommodate one geranylgeranyl group. Consistently, the crystal structure of doubly prenylated Ypt1:GDI complex reveals that one prenyl group is buried in the lipid-binding groove and forms extensive hydrophobic interactions, whereas the other prenyl group is situated on top of the first one and is largely exposed at the surface (Figure S19).[13a,15] These observations suggest that two prenyl groups have to bind sequentially to the GDI lipid-binding site. Based on these observations, we are able to conclude a working model of GDI-mediated Rab membrane recycling. The lipid-binding site of unbound GDI is closed to ensure the stability of the molecule in the cytosol. When GDI approaches prenylated Rab on the membrane, GDI first transiently associates with the Rab G-domain, leading to conformational changes on GDI and the opening of the lipid-binding site. The opened hydrophobic groove readily competes with membranes for the association with prenyl moieties. As a consequence, the first prenyl moiety is docked to GDI, followed by docking of the second one (Scheme 2).

Prompted by the success of Ypt1-GDI study, we further sought to trap the extremely weak KRas homodimer. Ras GTPases function as master regulators of a range of signal transduction pathways involved in diverse cellular processes. Oncogenic Ras genes are one of the most common oncogenes found in human tumors.[22] Recent studies suggested that the homodimerization of Ras proteins plays a critical role in Ras signaling.[23] However, because of the very weak and transient nature of the interaction, the access to Ras homodimer remains challenging.[24] To this end, KRas-thioester, N-Cys-KRas, KRas-BC and N-thioester-KRas were prepared (Figure S20,S21). The one-pot ligation led to covalent homodimer formation within 3 h (Figure S22). Further experiments showed that only C2C ligation yields KRas homodimer, but not N2C and N2N ligations (Figure S23). However, no C2C-ligated product was observed when the flexible C-terminal hypervariable region (HVR) of KRas is truncated (Figure S24). These results are consistent with the previous report that the HVR is required for homodimerization,[23a] suggesting that the C-termini of KRas could be in proximity in the homodimer.[25] Interestingly, KRas C2C ligation was only observed for GTP- and GDP-bound forms but not for GMP-bound form, suggesting homodimerization is dependent on the nucleotide binding state (Figure S24). The covalent KRas homodimer was purified by gel filtration (Figure S25). This is the first time to obtain unlipidated Ras homodimer.

In conclusion, we established a facile and unbiased strategy to trap weak protein–protein interactions using proximity-induced ligation. The covalent Ypt1-GDI complex allowed for elucidation of the mechanism of GDI-mediated Rab membrane recycling. This strategy also enabled us to trap the KRas homodimer, such trapping can be a useful tool to study Ras signaling. Moreover, the novel N2N and C2C ligation approaches contribute to new strategies for chemical protein modification. The presented method to trap weak

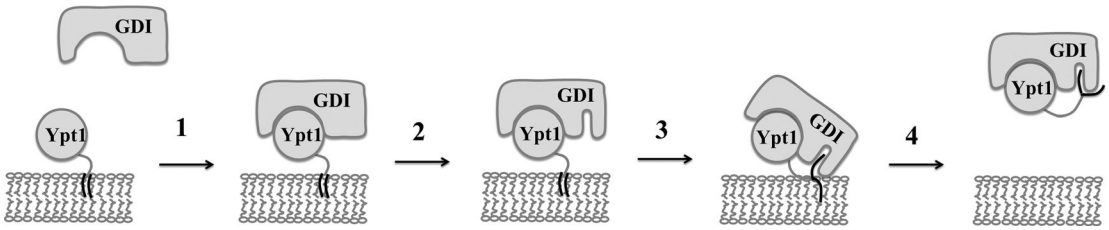

Scheme 2. Working model for GDI-mediated Rab membrane recycling. 1) Weak recognition, 2) Lipid-binding site opening, 3) Binding of the first prenyl group, 4) Binding of the second prenyl group.

protein–protein interactions opens up a new avenue to investigate protein interactions and the associated biological processes.

Acknowledgements

This work is supported by the funding from the Deutsche Forschungsgemeinschaft, DFG (grant No.: SPP 1623 and SFB 642) and European Research Council, ERC (ChemBioAP) to Y.W.W. C.E. is funded by the Kekulé Mobility Fellowship of the Chemical Industry Fund (FCI). O.K. is funded by the German Federal Ministry for Education and Research (Medizinische Chemie, TU Dortmund University, Grant No. BMBF 1316053).

Keywords: C-terminal 1,2-aminothiol · native chemical ligation · N-terminal thioester · protein–protein interactions · Ras homodimer

How to cite: *Angew. Chem. Int. Ed.* **2016**, *55*, 8129–8133
Angew. Chem. **2016**, *128*, 8262–8266

[1] a) A. Vinayagam, U. Stelzl, R. Foulle, S. Plassmann, M. Zenkner, J. Timm, H. E. Assmus, M. A. Andrade-Navarro, E. E. Wanker, *Sci. Signaling* **2011**, *4*, rs8; b) U. Stelzl, U. Worm, M. Lalowski, C. Haenig, F. H. Brembeck, H. Goehler, M. Stroedicke, M. Zenkner, A. Schoenherr, S. Koeppen, J. Timm, S. Mintzlaff, C. Abraham, N. Bock, S. Kietzmann, A. Goedde, E. Toksoz, A. Droege, S. Krobitsch, B. Korn, W. Birchmeier, H. Lehrach, E. E. Wanker, *Cell* **2005**, *122*, 957–968.

[2] M. E. Cusick, N. Klitgord, M. Vidal, D. E. Hill, *Hum. Mol. Genet.* **2005**, *14*, R171–R181.

[3] S. E. Ozbabacan, H. B. Engin, A. Gursoy, O. Keskin, *Protein Eng. Des. Sel.* **2011**, *24*, 635–648.

[4] a) J. Rudolph, *Nat. Rev. Cancer* **2007**, *7*, 202–211; b) J. R. Perkins, I. Diboun, B. H. Dessailly, J. G. Lees, C. Orengo, *Structure* **2010**, *18*, 1233–1243.

[5] M. Pelay-Gimeno, A. Glas, O. Koch, T. N. Grossmann, *Angew. Chem. Int. Ed.* **2015**, *54*, 8896–8927; *Angew. Chem.* **2015**, *127*, 9022–9054.

[6] a) D. F. Hansen, M. A. Hass, H. M. Christensen, J. Ulstrup, J. J. Led, *J. Am. Chem. Soc.* **2003**, *125*, 6858–6859; b) O. Vinogradova, J. Qin, *Top. Curr. Chem.* **2011**, *326*, 35–45.

[7] K. Melcher, *Curr. Protein Pept. Sci.* **2004**, *5*, 287–296.

[8] G. T. Hermanson, *Bioconjugate Techniques*, 2nd ed., Elsevier, Amsterdam, **2012**, pp. 215–342.

[9] M. A. Trakselis, S. C. Alley, F. T. Ishmael, *Bioconjugate Chem.* **2005**, *16*, 741–750.

[10] V. P. R. Chichili, V. Kumar, J. Sivaraman, *Protein Sci.* **2013**, *22*, 153–167.

[11] a) P. E. Dawson, T. W. Muir, I. Clark-Lewis, S. B. Kent, *Science* **1994**, *266*, 776–779; b) T. W. Muir, D. Sondhi, P. A. Cole, *Proc. Natl. Acad. Sci. USA* **1998**, *95*, 6705–6710.

[12] H. Stenmark, *Nat. Rev. Mol. Cell Biol.* **2009**, *10*, 513–525.

[13] a) O. Pylypenko, A. Rak, T. Durek, S. Kushnir, B. E. Dursina, N. H. Thomae, A. T. Constantinescu, L. Brunsveld, A. Watzke, H. Waldmann, R. S. Goody, K. Alexandrov, *EMBO J.* **2006**, *25*, 13–23; b) Y. W. Wu, K. T. Tan, H. Waldmann, R. S. Goody, K. Alexandrov, *Proc. Natl. Acad. Sci. USA* **2007**, *104*, 12294–12299.

[14] L. Yi, H. Sun, A. Itzen, G. Triola, H. Waldmann, R. S. Goody, Y. W. Wu, *Angew. Chem. Int. Ed.* **2011**, *50*, 8287–8290; *Angew. Chem.* **2011**, *123*, 8437–8440.

[15] A. Rak, O. Pylypenko, T. Durek, A. Watzke, S. Kushnir, L. Brunsveld, H. Waldmann, R. S. Goody, K. Alexandrov, *Science* **2003**, *302*, 646–650.

[16] Y. W. Wu, R. S. Goody, R. Abagyan, K. Alexandrov, *J. Biol. Chem.* **2009**, *284*, 13185–13192.

[17] K. Tripsianes, N. K. Chu, A. Friberg, M. Sattler, C. F. Becker, *ACS Chem. Biol.* **2014**, *9*, 347–352.

[18] Y. W. Wu, L. K. Oesterlin, K. T. Tan, H. Waldmann, K. Alexandrov, R. S. Goody, *Nat. Chem. Biol.* **2010**, *6*, 534–540.

[19] a) T. Sasaki, A. Kikuchi, S. Araki, Y. Hata, M. Isomura, S. Kuroda, Y. Takai, *J. Biol. Chem.* **1990**, *265*, 2333–2337; b) J. C. Sanford, J. M. Yu, J. Y. Pan, M. Wesslingresnick, *J. Biol. Chem.* **1995**, *270*, 26904–26909.

[20] a) O. Ullrich, H. Stenmark, K. Alexandrov, L. A. Huber, K. Kaibuchi, T. Sasaki, Y. Takai, M. Zerial, *J. Biol. Chem.* **1993**, *268*, 18143–18150; b) T. Soldati, M. A. Riederer, S. R. Pfeffer, *Mol. Biol. Cell* **1993**, *4*, 425–434.

[21] A. Ignatev, S. Kravchenko, A. Rak, R. S. Goody, O. Pylypenko, *J. Biol. Chem.* **2008**, *283*, 18377–18384.

[22] Y. Pylayeva-Gupta, E. Grabocka, D. Bar-Sagi, *Nat. Rev. Cancer* **2011**, *11*, 761–774.

[23] a) X. Nan, T. M. Tamguney, E. A. Collisson, L. J. Lin, C. Pitt, J. Galeas, S. Lewis, J. W. Gray, F. McCormick, S. Chu, *Proc. Natl. Acad. Sci. USA* **2015**, *112*, 7996–8001; b) W. C. Lin, L. Iversen, H. L. Tu, C. Rhodes, S. M. Christensen, J. S. Iwig, S. D. Hansen, W. Y. Huang, J. T. Groves, *Proc. Natl. Acad. Sci. USA* **2014**, *111*, 2996–3001.

[24] A. Dementiev, *Protein Expression Purif.* **2012**, *84*, 86–93.

[25] S. Muratcioglu, T. S. Chavan, B. C. Freed, H. Jang, L. Khavrutskii, R. N. Freed, M. A. Dyba, K. Stefanisko, S. G. Tarasov, A. Gursoy, O. Keskin, N. I. Tarasova, V. Gaponenko, R. Nussinov, *Structure* **2015**, *23*, 1325–1335.

Received: February 5, 2016
Revised: March 13, 2016
Published online: May 23, 2016

